



The role of extracellular potassium dynamics in the different stages of ictal bursting and spreading depression: A computational study

Gerson Florence^{a,b,c,*}, Markus A. Dahlem^d, Antônio-Carlos G. Almeida^b, José W.M. Bassani^a, Jürgen Kurths^{c,e,f}

^a Department of Biomedical Engineering, UNICAMP, Caixa Postal 6040, 13084-971 Campinas, SP, Brazil

^b Laboratory of Experimental and Computational Neuroscience, Department of Biomedical Engineering, Federal University of São João del-Rei, 36.301-160 São João del-Rei, MG, Brazil

^c Interdisciplinary Center for Dynamics of Complex Systems, University of Potsdam, Am Neuen Palais 19, D-14415 Potsdam, Germany

^d Institute for Theoretical Physics, Technological University of Berlin, Hardenbergstraße 36, D-10623 Berlin, Germany

^e Department of Physics, Humboldt University, Newtonstraße 15, D-12489 Berlin, Germany

^f Potsdam Institute for Climate Impact Research, PO Box 601203, D-14412 Potsdam, Germany

ARTICLE INFO

Article history:

Received 8 July 2008

Received in revised form

24 January 2009

Accepted 30 January 2009

Available online 7 February 2009

Keywords:

Extracellular potassium concentration

Excitability

Bifurcation

Ictal bursting

Spreading depression

ABSTRACT

Experimental evidences point out the participation of nonsynaptic mechanisms (e.g., fluctuations in extracellular ions) in epileptiform bursting and spreading depression (SD). During these abnormal oscillatory patterns, it is observed an increase of extracellular potassium concentration $[K^+]_o$ and a decrease of extracellular calcium concentration $[Ca^{2+}]_o$ which raises the neuronal excitability. However, whether the high $[K^+]_o$ triggers and propagates these abnormal neuronal activities or plays a secondary role into this process is unclear. To better understand the influence of extracellular potassium dynamics in these oscillatory patterns, the experimental conditions of high $[K^+]_o$ and zero $[Ca^{2+}]_o$ were replicated in an extended Golomb model where we added important regulatory mechanisms of ion concentration as Na^+-K^+ pump, ion diffusion and glial buffering. Within these conditions, simulations of the cell model exhibit seizure-like discharges (ictal bursting). The SD was elicited by the interruption of the Na^+-K^+ pump activity, mimicking the effect of cellular hypoxia (an experimental protocol to elicit SD, the hypoxia-induced SD). We used the bifurcation theory and the fast-slow method to analyze the interference of K^+ dynamics in the cellular excitability. This analysis indicates that the system loses its stability at a high $[K^+]_o$, transiting to an elevated state of neuronal excitability. Effects of high $[K^+]_o$ are observed in different stages of ictal bursting and SD. In the initial stage, the increase of $[K^+]_o$ creates favorable conditions to trigger both oscillatory patterns. During the neuronal activity, a continuous growth of $[K^+]_o$ by outward K^+ flow depresses K^+ currents in a positive feedback way. At the last stage, due to the depression of K^+ currents, the Na^+-K^+ pump is the main mechanism in the end of neuronal activity. Thus, this work suggests that $[K^+]_o$ dynamics may play a fundamental role in these abnormal oscillatory patterns.

© 2009 Elsevier Ltd. All rights reserved.

1. Introduction

In the cerebral tissue, there are different oscillatory patterns. Individual neurons typically present electrical activities as spiking and bursting (Izhikevich, 2007). However, in experimental models of brain slices these electrical activities can be altered with high increase of neuronal excitability. This situation happens during epileptiform bursting and spreading depression (SD). In interictal phase (between seizures), each neuron within an epileptic focus

has an electrical response called paroxysmal depolarizing shift (PDS). PDS consists of a large depolarization (20–40 mV) with 50–200 ms duration that triggers a burst of spikes, followed by an after hyperpolarization (Kandel et al., 2000). In an ictal event (seizure), cells depolarize as the PDS, but the bursting persists for seconds to tens of seconds (Xiong and Stringer, 2001). Another electrical activity is the SD discovered by Leão (1944). It is a slow wave that has been associated to migraine preceded by sensory hallucinations called aura (Gorji, 2001; Dahlem and Chroniclec, 2004). SD is characterized by large membrane depolarization (–20 to 0 mV) with spike inactivation and 1–2 min duration, propagating at velocities of a few mm/min to adjacent areas of the stimulated region (Müller and Somjen 2000; Martins-Ferreira et al., 2000).

* Corresponding author at: Department of Biomedical Engineering, UNICAMP, Caixa Postal 6040, 13084-971 Campinas, SP, Brazil. Tel.: +55 19 3521 9290; fax: +55 19 3289 3346.

E-mail address: florence@daad-alumni.de (G. Florence).

Despite of the differences between epileptiform bursting and SD, there are similarities in the process of neuronal excitability (Kager et al., 2000.). During seizures and also in SD, there are a decrease of extracellular calcium concentration ($[Ca^{2+}]_o$) and an increase of extracellular potassium concentration ($[K^+]_o$) (Heinemann et al., 1986; Nicholson 1980; Müller and Somjen, 2000). These changes in ionic concentration raise the cellular excitability (Pumain et al., 1985; Jensen and Yaari, 1997; Amzica et al., 2002; Cohen and Fields, 2004; Bikson et al., 1999), mainly because a decrease of $[Ca^{2+}]_o$ and an increase of $[K^+]_o$ depress the inhibitory mechanisms. Low $[Ca^{2+}]_o$ tends to block neurotransmitter release from active inhibitory interneurons (weakening synaptic transmission) and diminishes the hyperpolarization through a reduction in the calcium-activated potassium conductance. High $[K^+]_o$ decreases the K^+ driving force (difference between membrane potential and Nernst potential), lowering outward potassium currents (Pan and Stringer, 1997). It happens because high $[K^+]_o$ raises the Nernst potential of potassium (V_K), reducing the difference between membrane potential and V_K .

The basic notion about the influence of $[K^+]_o$ on the neuronal excitability is not new. Decades ago, Frankenhaeuser and Hodgkin (1956) initially observed that the potassium accumulates in interstitial space during repetitive stimulation of the squid giant axon which vanishes the hyperpolarizing after potential. In the same period, Grafstein (1956) presented the potassium hypothesis for SD. According to Grafstein's hypothesis, potassium releases into interstitial space would depolarize adjacent neurons, promoting SD propagation. Subsequently, Green (1964) and Fetziger and Ranck (1970) suggested that the potassium accumulation in the interstitial space during sustained neuronal activity could initiate and maintain epileptiform seizures. The central idea of the potassium accumulation hypothesis is that the raise of $[K^+]_o$ would trigger a regenerative process which high $[K^+]_o$ increases the neuronal excitability, leading to a spontaneous firing rate that, in turn, causes further raise of $[K^+]_o$ in a positive feedback way (Fetziger and Ranck, 1970).

While several studies have suggested that an increase of $[K^+]_o$ would only maintain the cellular hyperexcitability and not be involved in the seizure onset (Lux, 1974; Moody et al., 1974; Fisher et al., 1976; Heinemann et al., 1977; Somjen, 1979; Somjen et al., 1985) and SD onset (Somjen et al., 1992; Somjen, 2001, 2002; Herreras and Somjen, 1993; Herreras et al., 2005), it is still unclear whether $[K^+]_o$ can initiate seizures and SD. Hence, it is yet to be determined whether high $[K^+]_o$ is a primary factor of increased neuronal excitability or it is a secondary factor as a consequence of augmented neuronal firing (Somjen, 1979, 2001, 2002).

However, a series of studies have shown that the raise of $[K^+]_o$ may act as a primary factor of the cellular hyperexcitability. Changing the extracellular ionic milieu by the direct application of a high potassium solution can provoke seizures (Feldberg and Sherwood, 1957; Zuckermann and Glaser, 1968) and SD (Gorji, 2001). In hippocampal tissue slices, high $[K^+]_o$ in the bathing solution induces epileptiform bursting (Korn et al., 1987; Leschinger et al., 1993; Traynelis and Dingledine, 1988). Elevation of $[K^+]_o$ generates the transition from interictal to ictal discharges (Dichter et al., 1972; Jensen and Yaari, 1988; Borck and Jefferys, 1999) and further increase of $[K^+]_o$ elicits SD (Somjen, 2001). In solutions with low $[Ca^{2+}]_o$, the potassium diffusion between neighboring neurons can play an important role in the propagation and synchronization of the ictal discharges (Konnerth et al., 1984; Lian et al., 2001). Recently, single neuron and network models have shown the influence of $[K^+]_o$ in the modulation of paroxysmal activity (Bazhenov et al., 2004; Fröhlich et al., 2006), the nonsynaptic epileptiform activity (Park and Durand, 2006; Almeida et al., 2008), the neuronal synchronization (Park and Durand, 2006), the seizure afterdischarges (Kager et al., 2007) and

SD (Kager et al., 2000; Teixeira et al., 2008). In in-vitro experiments performed with hippocampal slices, elevated basal $[K^+]_o$ elicits ictal discharges (Jensen and Yaari, 1997). Therefore, besides the role of the $[K^+]_o$ during intense neuronal activity, these studies have evidenced the primary influence of high $[K^+]_o$ in the cellular hyperexcitability.

Hence, such evidences stand out the importance of nonsynaptic mechanisms in the transition to an elevated state of neuronal excitability (Feng and Durand, 2006). However, the extracellular potassium dynamics underlying the oscillatory patterns observed during seizure and SD remain poorly understood. Due to the restricted comprehension of the neuron biophysics and the lack of computational techniques, the propositions presented in early studies concerning the potassium accumulation hypothesis (e.g., Grafstein, 1956; Fetziger and Ranck, 1970) are oversimplified. Thus, the intention of this paper is to better understand the role of $[K^+]_o$ dynamics in these oscillatory patterns. This work analyzes cellular mechanisms of the CA1 pyramidal cells and explains their dynamic behaviors using the fast-slow analysis (Bertram et al., 1995) and bifurcation theory. Based on these studies, we suggest that the high $[K^+]_o$ may act as a primary factor of increased cellular excitability and influence the neuronal activity in the different stages of seizure discharges and SD.

2. Cell model

The cell model used here was based on the somatic, single-compartment model of the hippocampal region CA1 (for zero $[Ca^{2+}]_o$) proposed by Golomb et al (2006). The ionic currents ($\mu A/cm^2$) of the soma and of proximal dendrites are transient Na^+ current (I_{Na}), persistent sodium current (I_{NaP}), delayed rectifier K^+ current (I_{Kdr}), muscarinic-sensitive K^+ current (I_{KM}), A-type K^+ current (I_{KA}) and leak current (I_L). Other currents were added, pump current (I_{pump}), Na^+ and K^+ leak currents (I_{NaL} and I_{KL}) that determine the membrane potential in the resting state. The equations of these currents are given in Table 1. The calcium and Ca^{2+} -activated K^+ currents were not considered in this model, because we analyzed the neuronal excitability for zero $[Ca^{2+}]_o$. The variable V is the membrane potential, V_K and V_{Na} are the potassium and sodium Nernst potentials: $V_{ion} = 58 \log([ion]_o/[ion]_i)$, respectively. The gating variables are m , h , p , n , z , a and b (their equations are given in Table 2).

Na^+ - K^+ pump, glial buffering and ion diffusion have been used in network models to represent the extracellular potassium variations (Bazhenov et al., 2004; Park and Durand, 2006). Experimental studies have pointed out the influence of Na^+ - K^+ pump and glial buffering on extracellular potassium regulation and their possible implications on epileptic seizure and SD

Table 1

Currents of the cell-somatic model for high $[K^+]_{bath}$ and zero $[Ca^{2+}]_{bath}$ (hippocampal region CA1).

Currents ($\mu A/cm^2$)	Source
$I_{Na} = G_{Na} (V - V_{Na})$, where $G_{Na} = g_{Na} m^3 h$	(a)
$I_{NaP} = G_{NaP} (V - V_{Na})$, where $G_{NaP} = g_{NaP} p$	(a)
$I_{Kdr} = G_{Kdr} (V - V_K)$, where $G_{Kdr} = g_{Kdr} n^4$	(a)
$I_{KM} = G_{KM} (V - V_K)$, where $G_{KM} = g_{KM} z$	(a)
$I_{KA} = G_{KA} (V - V_K)$, where $G_{KA} = g_{KA} a^2 b$	(a)
$I_L = g_L (V - V_L)$	(a)
$I_{NaL} = g_{NaL} (V - V_{Na})$	(b)
$I_{KL} = g_{KL} (V - V_K)$	(b)
$I_{pump} = I_{NaPump} + I_{Kpump}$, where, $I_{Kpump} = -2 I_{max} A_{pump}$, $I_{NaPump} = 3 I_{max} A_{pump}$ $A_{pump} = (1 + 2.5/[K^+]_o)^{-2} (1 + 10.0/[Na^+]_i)^{-3}$	(b)

Source: (a) Golomb et al (2006) and (b) Kager et al. (2000).

Table 2Gating variables of the cell–somatic model for high $[K^+]_{\text{bath}}$ and zero $[Ca^{2+}]_{\text{bath}}$.

Gating variable	Kinetics/time constant (ms)	Parameters	Source
m	$m = m_{\infty}(V)$	$\theta_m = -30 \text{ mV}, \sigma_m = 9.5 \text{ mV}$	(a)
h	$dh/dt = (h_{\infty}(V) - h)/\tau_h(V)$, where $\tau_h(V) = 0.1 + 0.75/(1 + \exp(-(V+40.5)/-6))$	$\theta_h = -45 \text{ mV}, \sigma_h = -7 \text{ mV}$	(a)
p	$p = p_{\infty}(V)$	$\theta_p = -47 \text{ mV}, \sigma_p = 3 \text{ mV}$	(a)
n	$dn/dt = (n_{\infty}(V) - n)/\tau_n(V)$, where $\tau_n(V) = 0.1 + 0.5/(1 + \exp(-(V+27)/-15))$	$\theta_n = -35 \text{ mV}, \sigma_n = 10 \text{ mV}$	(a)
a	$a = a_{\infty}(V)$	$\theta_a = -50 \text{ mV}, \sigma_a = 20 \text{ mV}$	(a)
b	$db/dt = (b_{\infty}(V) - b)/15$	$\theta_b = -80 \text{ mV}, \sigma_b = -6 \text{ mV}$	(a)
z	$dz/dt = (z_{\infty}(V) - z)/75$	$\theta_z = -39 \text{ mV}, \sigma_z = 5 \text{ mV}$	(a)
	$X_{\infty}(V) = \{1 + \exp[-(V + \theta_x)/\sigma_x]\}^{-1}$, where $x = m, h, p, n, z, a, b$.		(a)

Source: (a) Golomb et al (2006).

Table 3Ion concentration flux of the cell–somatic model for high $[K^+]_{\text{bath}}$ and zero $[Ca^{2+}]_{\text{bath}}$.

Potassium concentration flux (mM/ms)	Source
$[K^+]_{\text{glial-buffering}} = k_1 ([B]_{\text{max}} - [B]_o) - k_2 [K^+]_o [B]_o$, where $K_2 = 0.0008/(1 + \exp(([K^+]_o - 15) / -1.09))$	(a) and (b)
$[\text{ion}]_{\text{bath diffusion}} = -([\text{ion}]_o - [\text{ion}]_{\text{bath}})/\tau_{\text{bs}}$	(c)
$[\text{ion}]_{\text{lateral diffusion}} = -([\text{ion}]_o - [\text{ion}]_i)/\tau_{\text{ss}}$	(c)
$[\text{ion}]_i (\text{currents}) = (I_{\Sigma(\text{ion})} 10^{-3} \text{Area}) / (F \text{Volume}_{\text{cell}})$, where $\text{Area} = 4\pi R^2$, $\text{Volume}_{\text{cell}} = 4\pi R^3/3$	(a)
$[\text{ion}]_o (\text{currents}) = -(I_{\Sigma(\text{ion})} 10^{-3} \text{Area}) / (F \text{Volume}_{\text{extracellular}})$, where $\text{Volume}_{\text{extracellular}} = Rv \text{Volume}_{\text{cell}}$	(a)

Source: (a) Kager et al. (2000); (b) Bazhenov et al. (2004); (c) Park and Durand (2006). In $[\text{ion}]_i (\text{currents})$ and $[\text{ion}]_o (\text{currents})$ equations, $I_{\Sigma(\text{ion}: K)}$ is $I_{\text{Kdr}}, I_{\text{KM}}, I_{\text{KA}}, I_{\text{KL}}$ plus I_{Kpump} and $I_{\Sigma(\text{ion}: Na)}$ is $I_{\text{NaTotal}}, I_{\text{Na}}, I_{\text{NaP}}, I_{\text{NaL}}$ plus I_{NaPump} . We multiplied by 10^{-3} to convert to ms. The $[\text{ion}]_{\text{bath diffusion}}$ is only considered in the equations of the first and last cells in the network.

(Haglund and Schwartzkroin, 1990; D'Ambrosio et al., 2002; D'Ambrosio, 2004; Benarroch, 2005; Takano et al., 2007). Hence, to simulate the ionic variations, we added these three mechanisms in the Golomb model. The equations of ionic regulations are given in Table 3. $[K^+]_{\text{glial-buffering}}$ is potassium concentration removed by glial cell from extracellular space, $[B]_o$ is free buffer extracellular concentration, $[\text{ion}]_{\text{lateral diffusion}}$ and $[\text{ion}]_{\text{bath diffusion}}$ are extracellular ion (K^+ , Na^+) concentrations originated from adjacent cells (lateral diffusion) and from the bath solution, respectively. $[\text{ion}]_i (\text{currents})$ and $[\text{ion}]_o (\text{currents})$ are intracellular and extracellular ion (K^+ , Na^+) concentrations, respectively, produced by Na^+ , K^+ and pump currents during neuronal activity. Here, in the one dimension network, the first and last cells are embedded in a bath solution with high $[K^+]_{\text{bath}}$ (8 mM/l), zero $[Ca^{2+}]_{\text{bath}}$ and normal $[Na^+]_{\text{bath}}$ (140 mM/l) and the other cell between them is only coupled by ion lateral diffusion (Fig. 1). Then, the membrane potential, gating variables, free buffer extracellular concentration and total extracellular and intracellular ion (K^+ , Na^+) concentrations can be expressed by the following differential equations (the parameters are given in Table 4):

$$dV/dt = -(I_{\text{Na}} + I_{\text{NaP}} + I_{\text{Kdr}} + I_{\text{KM}} + I_{\text{KA}} + I_{\text{L}} + I_{\text{NaL}} + I_{\text{KL}} + I_{\text{pump}})/C \quad (1)$$

$$dX/dt = (X_{\infty}(V) - X)/\tau_X(V), \quad \text{where } X : h, n, z, b \quad (2)$$

$$d[B]_o/dt = k_1 ([B]_{\text{max}} - [B]_o) - k_2 [K^+]_o [B]_o \quad (3)$$

$$d[K^+]_o/dt = [K^+]_{\text{glial-buffering}} + [K^+]_{\text{lateral diffusion}} + [K^+]_{\text{bath diffusion}} + [K^+]_{\text{o(currents)}} \quad (4)$$

$$d[Na^+]_o/dt = [Na^+]_{\text{lateral diffusion}} + [Na^+]_{\text{bath diffusion}} + [Na^+]_{\text{o(currents)}} \quad (5)$$

$$d[K^+]_i/dt = [K^+]_{\text{i(currents)}} \quad (6)$$

$$d[Na^+]_i/dt = [Na^+]_{\text{i(currents)}} \quad (7)$$

The analyses of this model focused on effects of high $[K^+]_o$ on the neuron behavior. In the simulation of ictal bursting, using a bath solution with high $[K^+]_{\text{bath}}$, the raise of basal extracellular potassium concentration is initially promoted by K^+ diffusion from the bath solution to the interstitial space of the first and last neurons in the network and, in sequence, by K^+ lateral diffusion from one neuron to the neighbor neuron, increasing the cellular excitability. Afterwards, $[K^+]_o$ raises more during intense neuronal activity which increases the cellular excitability in a positive feedback way and spreads this high $[K^+]_o$ by lateral diffusion to adjacent neurons. In other simulation, using an experimental protocol to elicit SD (Somjen, 2001), the transition from bursting to SD was simulated by the blockage of $Na^+ - K^+$ pump current. In this case, there is an initial deep raise of $[K^+]_o$ that it is also maintained afterwards by a positive feedback way between the neuronal activity and the raise of $[K^+]_o$. Then, the high $[K^+]_o$ diffuses by lateral diffusion to adjacent neurons. To better understand the effects of high $[K^+]_o$ on these abnormal oscillatory patterns, in the dynamic analysis we used the fast–slow method (Hoppensteadt and Izhikevich, 1997) and bifurcation theory. $[K^+]_o$ varies on a slow time-scale. Therefore, we could treat $[K^+]_o$ as a parameter in the bifurcation analysis (Fröhlich et al., 2006; Fröhlich and Bazhenov, 2006), interrupting the regulatory mechanisms of $[K^+]_o$. This reduction of the full model allowed a detailed bifurcation analysis, evaluating the neuron behavior for different levels of $[K^+]_o$ within the physiological range. All bifurcation diagrams were calculated by using the software XPP-AUTO (Ermentrout, 2002).

Further bifurcation analysis was performed to understand the role of $Na^+ - K^+$ pump current (I_{pump}) in the slow modulation of ictal bursting and SD dynamic behaviors within the conditions of high $[K^+]_{\text{bath}}$ and low $[Ca^{2+}]_{\text{bath}}$. Concerning the slow modulation of neuronal activities, the fast–slow method is frequently applied to analyze the mechanism that terminates the neuronal activity (Hoppensteadt and Izhikevich, 1997). In general, the bursting consists of oscillations with two time scales: fast currents that modulate spiking oscillation within a burst and slow currents which modulate the slow oscillation between bursts (Izhikevich, 2007). Muscarinic-sensitive K^+ current in zero $[Ca^{2+}]_o$ (Golomb et al., 2006) and Ca^{2+} -activated K^+ currents in normal $[Ca^{2+}]_o$ (Fröhlich and Bazhenov, 2006) are examples of burst slow modulation in nonsynaptic neuronal activity. However, other studies point out the role of $Na^+ - K^+$ pump current in the modulation of seizure discharges (Kager et al., 2007; Almeida et al.,

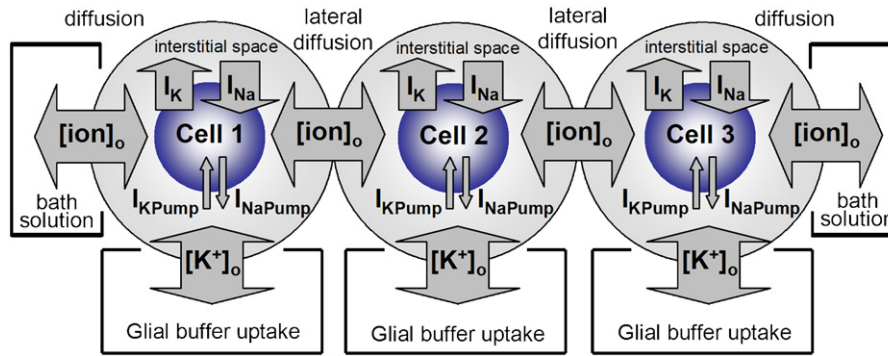


Fig. 1. Schematic diagram of the model. This schematic diagram was based on the configuration of cell model proposed by Park and Durand (2006), considering the cell shape as a sphere and three mechanisms of potassium regulation: $\text{Na}^+\text{-K}^+$ pump, glial buffering and ion diffusion. Here, there are three neurons within one dimension network. Each neuron is involved by interstitial space. The first and last cells are embedded in a bath solution with high $[\text{K}^+]_{\text{bath}}$ (8 mM/l), zero $[\text{Ca}^{2+}]_{\text{bath}}$ and normal $[\text{Na}^+]_{\text{bath}}$ (140 mM/l). The middle cell is only coupled to adjacent cells by ion lateral diffusion. Thus, potassium and sodium ions can diffuse between the bath solution and the interstitial space (diffusion) and inside interstitial spaces (lateral diffusion). The I_K , I_{Na} , I_{Kpump} , I_{Napump} correspond to potassium, sodium, pump currents, respectively. Potassium and sodium ions can accumulate in the interstitial space and within the cell.

Table 4

Parameters of the cell–somatic model for high $[\text{K}^+]_{\text{bath}}$ and zero $[\text{Ca}^{2+}]_{\text{bath}}$.

Parameters	Source	
g_{Na}	Transient Na^+ conductance	35 mS/cm ² (a)
g_{NaP}	Persistent sodium conductance	0.3 mS/cm ² (a)
g_{Kdr}	Delayed rectifier K^+ conductance	6 mS/cm ² (a)
g_{M}	Muscarinic-sensitive K^+ conductance	1 mS/cm ² (a)
g_{A}	A-type K^+ conductance	1.4 mS/cm ² (a)
g_{LNa}	Na^+ leakage conductance	0.0548 mS/cm ² (b)
g_{LK}	K^+ leakage conductance	0.1374 mS/cm ² (b)
g_{L}	Leakage conductance	0.2 mS/cm ² (c)
V_{L}	Leakage Nernst potential	−70 mV (a)
C	Soma capacitance	1 $\mu\text{F}/\text{cm}^2$ (a)
I_{max}	Pump maximal current	63 $\mu\text{A}/\text{cm}^2$ (d)
$[B]_{\text{max}}$	Maximal buffer capacity	265 mM/l (e)
K_1	Rate constant of buffer mechanism	0.0008 (c)
τ_{ss}	Lateral diffusion time constant	20 ms (e)
τ_{bs}	Diffusion time constant	240 ms (d)
F	Faraday's constant	96.49 C/mMol (f)
R_V	Volume ratio (= Volume _{extracellular} /Volume _{cell})	0.15 (e)
R	Radius of cell	8.9×10^{-4} cm (e)
$[\text{K}^+]_{\text{bath}}$	K^+ concentration in the bath	8 mM/l (e)
$[\text{Na}^+]_{\text{bath}}$	Na^+ concentration in the bath	140 mM/l (c)

Source: (a) Golomb et al. (2006); (b) Kager et al. (2007); (c) Kager et al. (2000); (d) modified values; (e) Park and Durand (2006) and (f) definition. In the transition from ictal bursting to SD, we used $\tau_{\text{bs}} = 18 \times 10^3$ to decrease the influence of the bath solution. Since the network has few neurons, the bath solution absorbs the potassium from the extracellular space, limiting the raise of $[\text{K}]_o$ during the spreading depression.

2008) and SD (Kager et al., 2000). In this case, high $[\text{K}^+]_o$ impairs potassium currents to end the neuronal activity. Therefore, within these conditions, the negative current (electrogenic effect) produced by the pump current (I_{pump}) plays a role in cellular repolarization.

3. Epileptiform bursting dynamics

The dynamic analysis of epileptiform bursting involves different aspects such as alterations in cellular components (e.g., ionic concentrations) which are determinant to the behavior of each neuron within the network, the propagation of cellular activity and neuronal synchronization in a global network behavior. Here, this first aspect was analyzed, studying the effects of high $[\text{K}^+]_o$ on the different stages of the abnormal neuron activity. We simulated the cell model containing high $[\text{K}^+]_{\text{bath}}$

(8mM/l) and zero $[\text{Ca}^{2+}]_{\text{bath}}$. Herewith, it was possible to elicit seizure-like discharges (ictal bursting) without any external stimulus, as seen in Fig. 2(a). In this case, the high extracellular K^+ concentration ($[\text{K}^+]_o$) raises the cellular excitability in each neuron within the network, creating the conditions to produce ictal bursts. On the other hand, the pump current (I_{pump}) acts to repolarize the cell, finishing the bursting after some seconds.

The effects of $[\text{K}^+]_o$ and I_{pump} in the neuronal behavior are shown in the bifurcation diagrams (Fig. 3). In the Fig. 3(a), the $[\text{K}^+]_o$ was considered as a control parameter of the cellular excitability. At normal $[\text{K}^+]_o$, the cell stays in the resting state (stable branch of equilibrium points). With the raise of $[\text{K}^+]_o$, the neuron becomes more excitable, reaching the bifurcation point FB where the system shifts from the resting state to the ictal bursting regime (limit cycle branch). The other studied case is shown in the Fig. 3(b). Here, the bifurcation diagram presents a z-shaped line of equilibrium points as a function of I_{pump} which provides a slow modulation of the ictal bursting. Along the z-shaped line, three bifurcation points are identified. These points determine the transitions to different ictal bursting stages. The transition from the resting state to the repetitive spiking (limit cycle attractor) happens via a fold bifurcation. During the bursting, the changes in spiking amplitude and frequency happen via a supercritical Hopf bifurcation. At the end of bursting, the repetitive spiking disappears via a saddle homoclinic orbit bifurcation, returning to the resting state. Then, the bursting starts again following a typical hysteresis loop (Izhikevich, 2007) between the resting state (stable branch of equilibrium points) and the bursting (limit cycle branch).

In the first stage of the ictal bursting, the membrane potential (V) increases slowly as an indirect effect of the K^+ diffusion from the bath solution with high potassium concentration to the cellular interstitial space. The K^+ diffusion provokes a gradual growth of $[\text{K}^+]_o$, depressing the potassium leak current (I_{KL}). The consequence of low I_{KL} is an unbalance between the currents responsible for the cellular resting state. This current unbalance produces a positive resultant current ($dV/dt = -(-I_R)/C$, $I_R = \sum I_{\text{cell}}$ currents). Then, the positive I_R causes an initial augment of V . During this process, the persistent sodium current (I_{NaP}) is activated, producing a fast growth of V that culminates in the bursting eruption, as seen in Fig. 4(a). Thus, with the augment of $[\text{K}^+]_o$, the membrane potential becomes more depolarized, creating the conditions to the bursting eruption. This happens at a $[\text{K}^+]_o$ of 6.688 mM/l where the stable equilibrium coalesces with an unstable equilibrium, annihilating each other via a fold

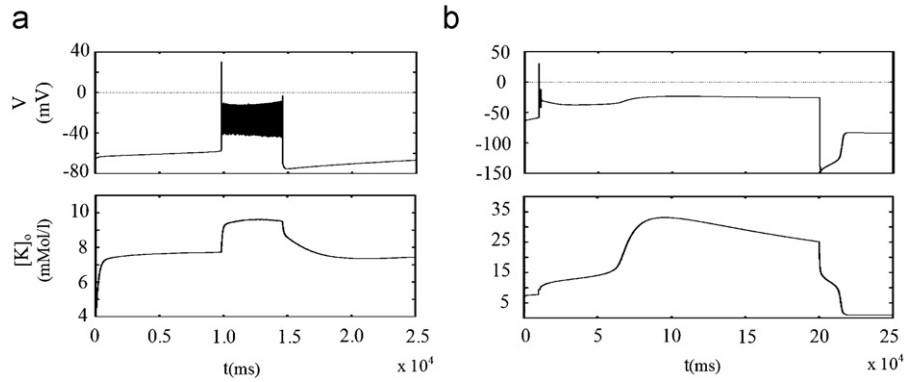


Fig. 2. Membrane potential (V) and extracellular potassium concentration $[K^+]_o$: (a) in this simulation with $[K^+]_{bath} = 8$ mMol/l, seizure like-discharges persist for 0.5×10^4 ms and (b) the transition from bursting to SD occurs when we interrupt pump current in $t = 1.1 \times 10^4$ ms. In $t = 20.0 \times 10^4$ ms, pump activity is restored, finishing SD. In both situations, the initial increase of $[K^+]_o$ is provoked by K^+ diffusion and during neuron activities the high increase of $[K^+]_o$ is caused by K^+ currents.

bifurcation (Fig. 3(a)). Straight afterward, the trajectory jumps up to the limit cycle attractor corresponding to repetitive spiking.

About the second stage, after each spike the I_{NaP} elevates V , activating the I_{Na} to produce a new spike. Thus, the I_{NaP} continuously triggers the spikes within the bursting regime. Here, the interplay between I_{NaP} and depressed K^+ currents (caused by high $[K^+]_o$) results in an increase of the spike frequency and a decrease of the spike amplitude. The variations of frequency and amplitude can be explained by the difficulty of depressed K^+ currents to reduce the level of membrane potential after each spike in opposition to I_{NaP} . In this case, a new spike will initiate earlier (increasing the spike frequency) when the conductance of I_{Kdr} is still high (decreasing the spike amplitude) (Fig. 4(b)). Nevertheless, during the bursting, the conductance of I_{KM} slowly increases, reducing the effect of I_{NaP} (Fig. 4(c)). Herewith, the I_{KM} diminishes the level of the membrane potential between spikes, decreasing the frequency and increasing the amplitude by a supercritical Hopf bifurcation (Fig. 3(b)). However, due to the high $[K^+]_o$, the I_{KM} is not strong enough to generate a negative I_R within interspike intervals. Hence, the bursting continues for seconds.

As shown before, the high $[K^+]_o$ acts as a primary factor of neuronal excitability, since it creates the conditions to elicit the ictal bursting. Furthermore, our simulations yield that it also raises the cellular excitability in a positive feedback way (McCormick and Contreras, 2001). With high $[K^+]_o$, the depressed K^+ currents can not interrupt the bursting. The elevated membrane potential allows the K^+ channels to remain open all time during the bursting, leading to a continuous growth of $[K^+]_o$, as seen in the Fig. 2(a). Then, in a feedback way, the continuous growth of $[K^+]_o$ will provoke further depression of K^+ currents. Herewith, the $[K^+]_o$ increases from 6.688 mMol/l to around 10 mMol/l (the “ceiling” level). This state of increased neuronal excitability changes in the last stage of ictal bursting (Fig. 4(d)), when the mechanisms of K^+ regulation slowly decrease $[K^+]_o$. Here, the I_{pump} plays an important role. The Na^+-K^+ pump begins to restore ion concentrations (reducing $[K^+]_o$) and also to produce a negative resultant current sufficiently to deactivate the voltage-sensitive channels. The bursting finishes when the I_{pump} overcomes the effect of I_{NaP} , producing a negative I_R within interspike intervals that will hyperpolarize the membrane potential. In this moment, the limit cycle branch contacts the unstable branch at a saddle point (Fig. 3(b)) and becomes a homoclinic orbit. At last, the I_{pump} provides the system to cross the stable manifold of this saddle point, and then the ictal bursting disappears by a saddle homoclinic orbit bifurcation (Izhikevich, 2007). After this bifurcation, the membrane potential jumps down to the resting state, completing the hysteresis loop.

4. The transition to SD

The transition from bursting to SD was simulated by reducing I_{NaPump} and I_{Kpump} to zero and this resulted in a SD-like depolarization (Fig. 2(b)). The reduction of the Na^+-K^+ pump activity is an experimental protocol to elicit SD (Somjen, 2001). With an interruption of pump currents, the K^+ recovery is impaired, causing a raise of $[K^+]_o$ above the “ceiling” level that will induce SD. Afterwards, the Na^+-K^+ pump activity is restored, ending the SD. These effects of $[K^+]_o$ and I_{pump} in the neuronal behavior are shown in Figs. 3(a) and (c). In Fig. 3(a), the raise of $[K^+]_o$ above the “ceiling” level changes the neuronal behavior. It happens at a $[K^+]_o = 15.86$ mMol/l, when the limit cycle disappears via a supercritical Hopf bifurcation, inactivating the spikes. In Fig. 3(c), the bifurcation diagram presents a z-shaped line of equilibrium points where two stable branches are separated by an unstable branch. In this diagram, with the increase of I_{pump} , the membrane potential is repolarized, ending the SD via a fold bifurcation.

The first stage of SD is characterized by the spike inactivation (Fig. 5(a)), keeping some similarities with the second stage of the ictal bursting (Fig. 4(b)). However, without pump currents, the $[K^+]_o$ raises faster. Herewith, the high $[K^+]_o$ causes a large depression in the K^+ driving force which reduces the influences of the I_{KM} in the membrane repolarization. Thus, there are an increase of the spike frequency and a decrease of the spike amplitude, culminating in the spike inactivation by a supercritical Hopf bifurcation (Fig. 3(a)). After this bifurcation, the system shifts from the ictal bursting to the SD.

The next stage is a slow membrane depolarization provoked by a small positive I_R (Fig. 5(b) and (c)). After the spike inactivation process, the delay between I_{Na} and I_{Kdr} oscillations disappears, but both continuously activated, decreasing gradually their amplitudes. In addition, the total Na^+ currents ($I_{NaTotal}$) overcome the total K^+ currents (I_{KTotal}), producing a positive I_R which will slowly depolarize V . During this process, the SD is maintained by a positive feedback between increasing $[K^+]_o$ and membrane depolarization. This raises the delayed rectifier K^+ conductance (G_{Kdr}) which releases even more K^+ . This situation changes in the third stage when the Na^+-K^+ pump is activated (Fig. 5(d)). Here, the Na^+-K^+ pump restores ion concentrations and also generates a negative I_R that deactivates all voltage-sensitive channels, ending the SD by a fold bifurcation.

5. Discussion

Simulations of neuron models have shown possible effects of $[K^+]_o$ in the epileptiform activity and SD. These effects are related

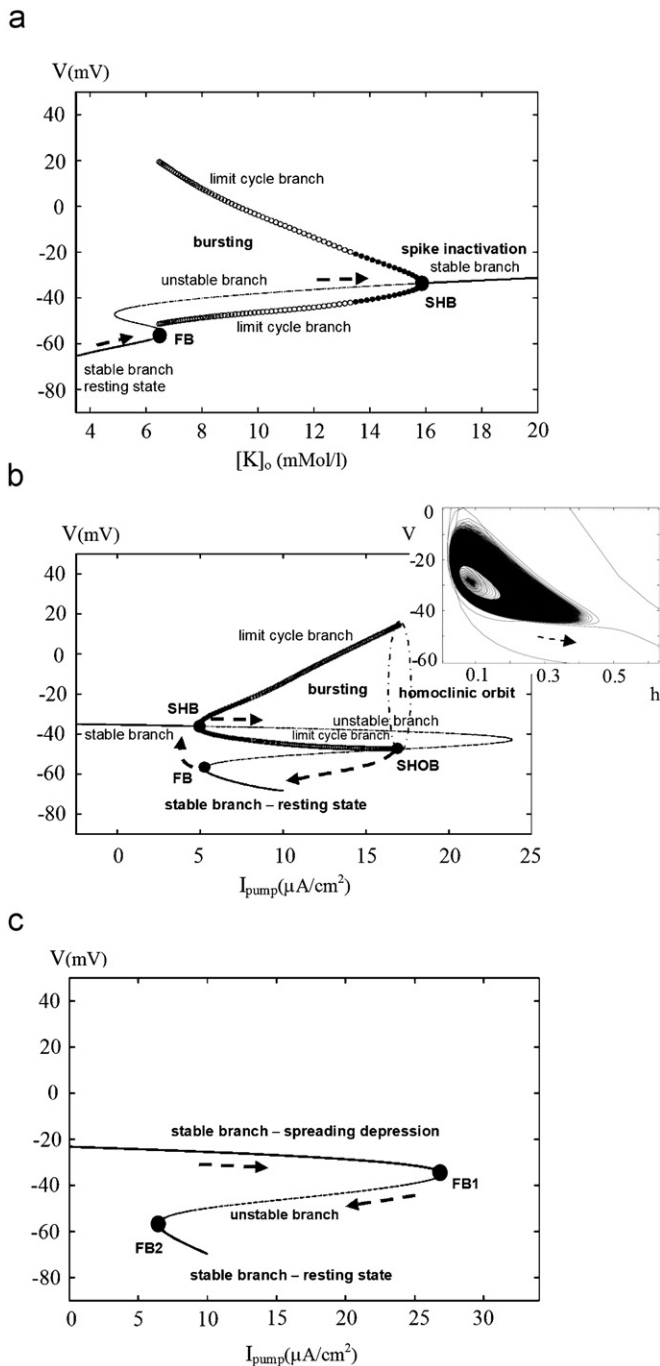


Fig. 3. Bifurcation diagrams: (a) the raise of $[K^+]_o$ causes two bifurcations. First one is a fold bifurcation (at the point marked FB) that determines the transition from the resting state to the bursting regime. Second one is a supercritical Hopf bifurcation (at the point marked SHB), when the SD initiates, (b) the I_{pump} provides a slow modulation of the ictal bursting. Here, three bifurcations happen along the z-shaped line, fold bifurcation (at the point marked FB) in the transition to limit cycle, supercritical Hopf bifurcation (at the point marked SHB) during the bursting and saddle homoclinic orbit bifurcation (at the point marked SHOB) in the transition to the resting state. This diagram was performed for $[K^+]_o = 9.5$ mMol/l. In the right corner, the phase space (V , h_{fast} Na channel) shows the increasing limit cycle causes by the augment of I_{pump} until the transition to the resting state and (c) along the z-shaped line, there are two bifurcation points, FB1 and FB2. The I_{pump} finishes the SD (upper stable branch) via fold bifurcation (at the point marked FB1), returning the system to the resting state (lower stable branch). In this case, it was considered $[K^+]_o = 35$ mMol/l.

with the modulation of paroxysmal activity (Bazhenov et al., 2004; Fröhlich et al., 2006), the neuron synchronization (Park and Durand, 2006), the increasing neuronal excitability via the

chloride Nernst potential overcoming the membrane potential as a consequence of the high $[K^+]_o$ (Almeida et al., 2008) and via a positive feedback between rising $[K^+]_o$ and the neuron activity during seizure after discharges (Kager et al., 2007) and SD (Kager et al., 2000). Furthermore, Teixeira et al. (2008) proposes a critical condition for the wave propagation during SD which the total K^+ currents have to overcome the I_{Kpump} earlier than the total Na^+ currents become smaller than the I_{NaPump} . In this paper, simulating a model of hippocampal region CA1 containing high $[K^+]_{bath}$ and zero $[Ca^{2+}]_{bath}$ and using the bifurcation theory and fast-slow method in reduced model we suggest that the extracellular potassium dynamics may play an important role in the different stages of ictal bursting and SD. Although epileptic seizures are understood as abnormal function of complex neuronal nets and only the brain as a whole can produce real convulsions, the brain could not malfunction without some abnormality of its elements (Kager et al., 2007). Neurons are basic units of the brain and analyzing the effects of altered cellular components on the dynamics of neuron behavior is crucial for understanding the organism operation during anomalous neuronal oscillatory patterns. Hence, three important points are shown here. First, in the initial stage the model simulations and the bifurcation analysis indicate that high $[K^+]_o$ may act as a primary factor of increased neuronal excitability. Second, during the neuronal activity neurons present a complex behavior determined by the interactions between the fast and slow currents. The depression of K^+ currents caused by high $[K^+]_o$ changes the neuron behavior to produce abnormal oscillatory patterns. Moreover, the depressed K^+ currents are not strong enough to terminate the neuronal activity. Within these conditions, the electrogenic current of Na^+K^+ pump may be an important mechanism in the modulation of these abnormal neuronal activities. Third, specific mechanisms may act to increase the excitability and modulate the neuronal activity in both oscillatory patterns, suggesting that there could be an underlying mechanistic similarity common to epilepsy and migraine preceded by aura.

5.1. High $[K^+]_o$ as a primary factor of increased neuronal excitability

It is well established that the $[K^+]_o$ dynamics influence the neuronal excitability in a positive feedback between rising $[K^+]_o$ and neuronal depolarization (Fröhlich et al., 2006). This positive feedback mediated by elevated $[K^+]_o$ plays an important role during seizure discharges and SD (Kager et al., 2000). Nevertheless, there is a controversy about the primary function of $[K^+]_o$ in the neuronal excitability (Herreras et al., 2005). The SD and ictal bursting are usually not preceded by K^+ oscillations, as seen in the Fig. 2. Hence, the absence of a prior deep variation in $[K^+]_o$ seems to refute the idea that increasing $[K^+]_o$ provides the eruption of ictal bursting and SD (Somjen, 1979, 2002). However, in our studies with high $[K^+]_{bath}$, the K^+ diffusion causes an augment of the basal extracellular K^+ concentration that produces a slow cell depolarization. The initial cell depolarization shifts the membrane potential closer to the firing threshold. At this moment, the Na^+ voltage-sensitive currents (I_{NaP} and I_{Na}) are activated, starting the ictal bursting. Yet, increasing more the $[K^+]_o$, the SD can be elicited. Therefore, besides the positive feedback effect of potassium during the neuronal activity, our work suggests that a high $[K^+]_o$ may act as a primary factor of increased neuronal excitability, creating favorable conditions to trigger seizure discharges and SD.

The effects of $[K^+]_o$ in the neuron behavior are uncovered in the bifurcation diagram of Fig. 3(a). With augment of $[K^+]_o$, the system loses its stability via a fold bifurcation when the resting state disappears to start the ictal bursting regime. In addition, the

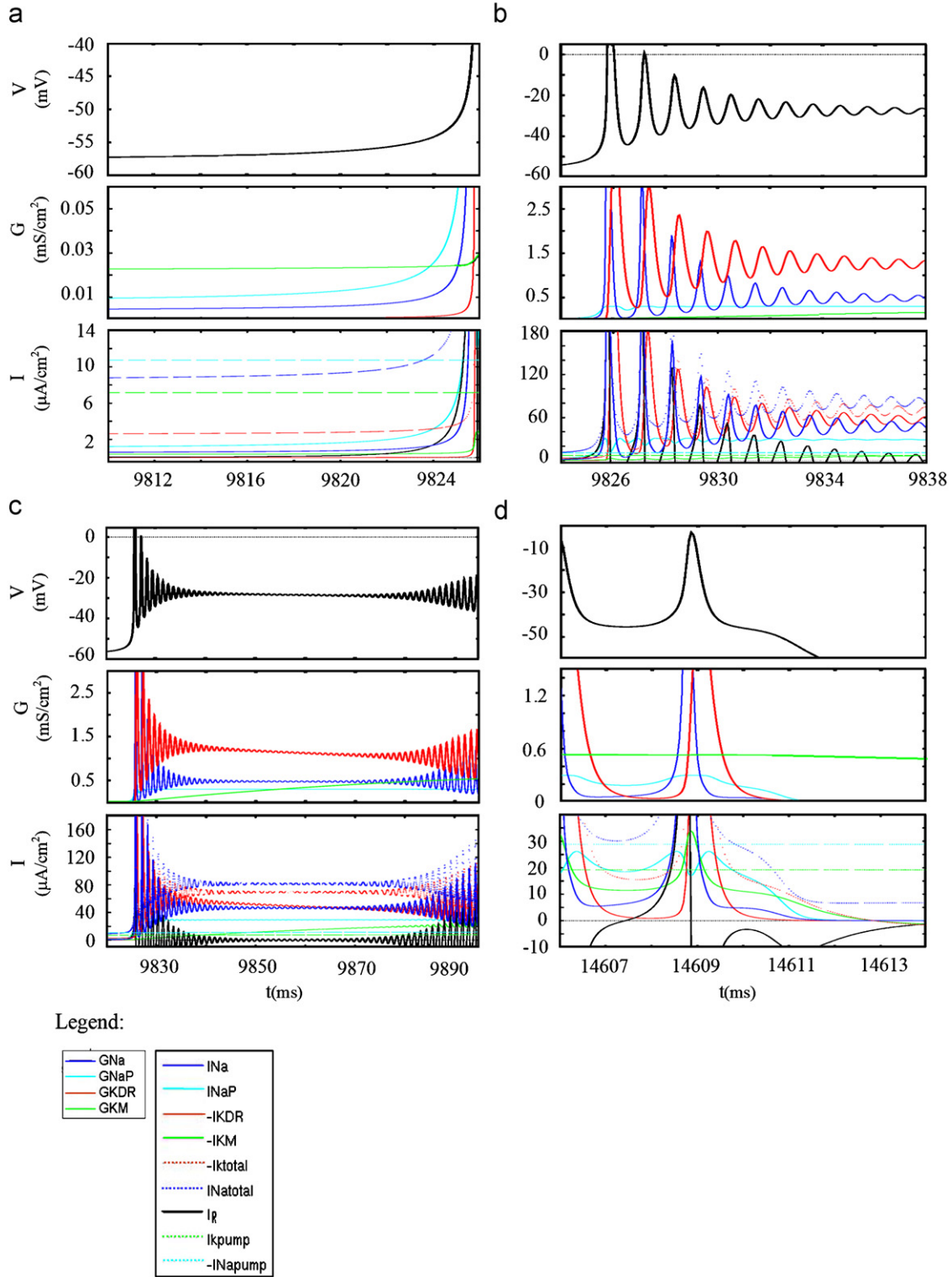


Fig. 4. Different stages of the ictal bursting. To facilitate the analysis, we plotted the absolute values of K^+ , Na^+ and pump currents, multiplying the negative currents by $(-)$ 1: (a) in first stage, the depressed K^+ currents by high $[K^+]_o$ provoke a positive I_R (due to the depression of K^+ currents, the absolute value of Σ positive currents becomes higher than absolute value of Σ negatives currents, $|I_{Natotal}+I_{Kpump}| > |(-)I_{Napump}+(-)I_{Ktotal}+(-)I_L|$). Then, this positive I_R raises the membrane potential (V). If we compare I_{Napump} and I_{Kpump} with $I_{Natotal}$ and I_{Ktotal} , the pump currents are higher than Na^+ and K^+ currents. However, the $\Sigma(I_{Kpump}+(-)I_{Ktotal}+(-)I_{Napump}+I_{Natotal})$ produces a positive resultant current, because $|I_{Kpump}+(-)I_{Ktotal}| > |(-)I_{Napump}+I_{Natotal}|$. With the raise of V , the I_{NaP} is activated. At this moment, the ictal bursting is triggered. Herewith, the $I_{Natotal}$ overcomes the I_{Napump} , (b) the activation of I_{NaP} elicits a train of spikes, during the active state of the neuron, (c) during second stage, the G_{KM} increases slowly, reducing the effect of I_{NaP} but not enough to finish the bursting and (d) In the last stage, I_{pump} ($I_{pump} = I_{Napump} - I_{Kpump}$) is the main current which causes a negative I_R (because $|(-)I_{Napump}+(-)I_{Ktotal}+(-)I_L| > |I_{Natotal}+I_{Kpump}|$) within the interspike intervals that finishes the bursting.

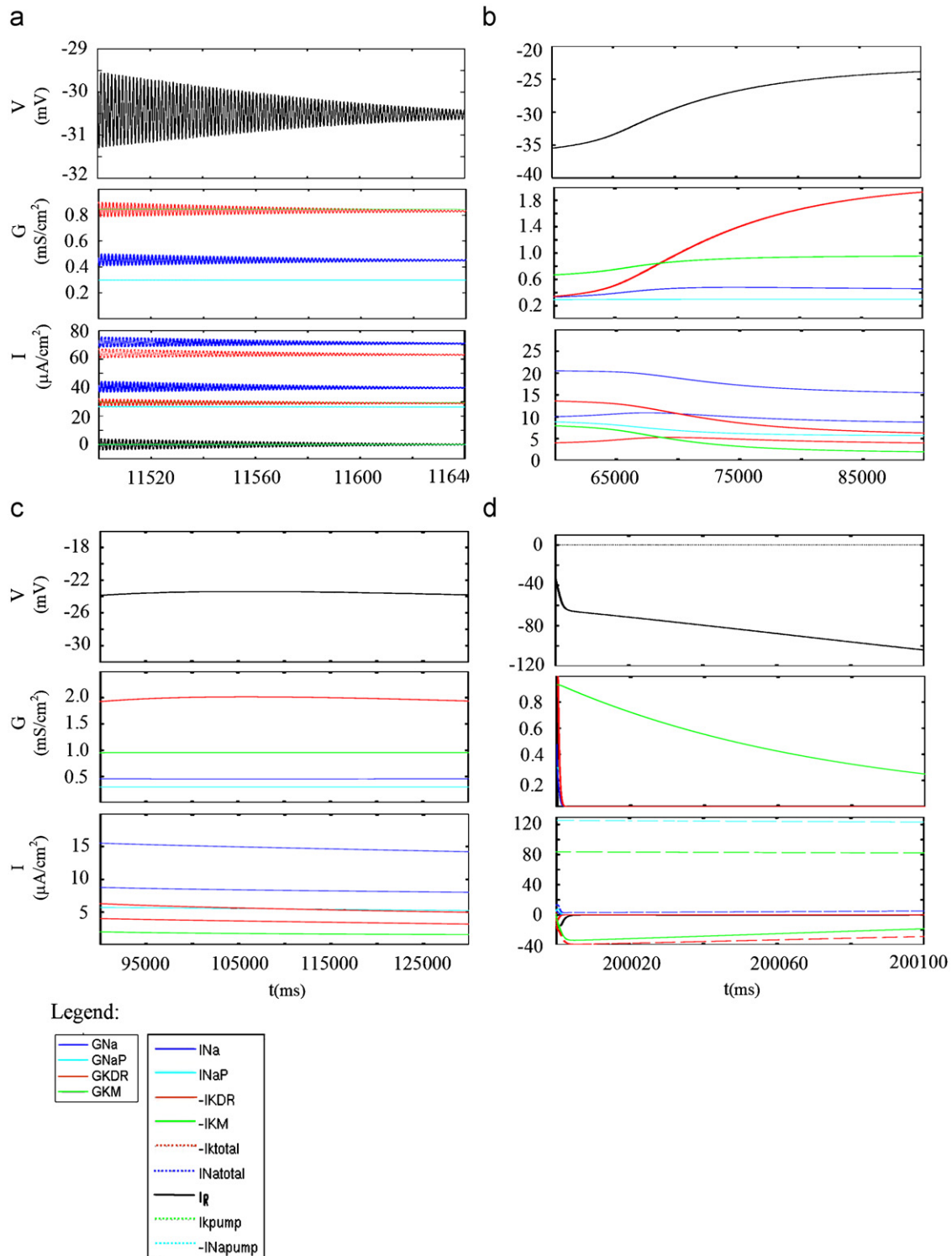


Fig. 5. Different stages of SD elicited by interruption of pump activity. As the Fig. 4, we plotted the absolute values of K^+ , Na^+ and pump currents, multiplying the negative currents by (-1) : (a) in first stage, the G_{Kdr} remains elevated, hindering the spike oscillations. (b), (c) in second stage, the Na^+ and K^+ currents continue activated, producing a small positive I_R (because $|I_{Na\text{total}}| > |I_{K\text{total}}|$) that slowly depolarizes the neuron and (d) pump activity is restored, finishing SD. In this stage, due to $V < V_K$, K^+ currents become positive (here, K^+ currents appear negative, because in all figures we multiplied the negative currents by (-1)). Then, I_{pump} is the only negative current that acts to finish the SD.

continuous growth of $[K^+]_o$ inactivates the spikes and elicits the SD via a supercritical Hopf bifurcation. In this case, the growth of $[K^+]_o$ happens with the interruption of the $Na^+ - K^+$ pump activity. Within this condition, the $[K^+]_o$ can raise in a positive feedback manner, allowing a slow depolarization with spike inactivation that characterizes the SD wave.

5.2. Alterations in the neuron behavior by the depressed K^+ currents and the modulation of neuronal activity by the $Na^+ - K^+$ pump

The ictal bursting shows a complex behavior determined by the interactions between specific cellular mechanisms. The first stage of the ictal bursting is characterized by a slow increase of V

caused by K^+ diffusion. Here, the K^+ diffusion depresses the I_{KL} , raising the neuronal excitability. During the bursting, the I_{NaP} guarantees a level of cellular depolarization above the firing threshold that allows a repetitive spiking (within the limit cycle attractor). The interactions between the I_{NaP} and the I_{KM} influence the spike amplitude and frequency. Moreover, the I_{Na} and the I_{Kdr} play an important role in the spike modulation (the I_{Na} causes a fast raise of V , and after the I_{Kdr} produces the decline of V). In the last stage of ictal bursting, due to the high $[K^+]_o$, the depressed I_{KM} is not strong enough to finish the seizure discharges. At this moment, the Na^+-K^+ pump restores the ion concentrations and produces a negative I_R within interspike intervals that will end the bursting. In all these stages, the K^+ currents directly influence the neuron activity. Thus, the depression of K^+ currents by high $[K^+]_o$ provokes a profound alteration in the neuronal behavior that results in an abnormal oscillatory pattern.

Experimental and theoretical works have demonstrated that brief bursts (50–200 ms) typically associated to the interictal phase (Kandel et al., 2000; Xiong and Stringer, 2001) are modulated by K^+ currents in nonsynaptic neuronal activity, e.g., I_{KM} in zero $[Ca^{2+}]_o$ (Golomb et al., 2006) and Ca^{2+} -activated K^+ currents in normal $[Ca^{2+}]_o$ (Fröhlich and Bazhenov, 2006). Nevertheless, other studies have emphasized the importance of Na^+-K^+ pump in the modulation of seizure discharges (Kager et al., 2007; Almeida et al., 2008) and SD (Kager et al., 2000). Our simulations confirm these studies and our dynamic analyses explain how the I_{pump} may modulate the neuron behavior and determine their stages. Here, the bifurcation points define the transitions between three different stages during the ictal bursting. In the first one, the neuron leaves the resting state via a fold bifurcation with a decreasing of I_{pump} which raises the neuronal excitability. The second stage has a similar scenario shown in the Golomb model. There, the Hopf bifurcation point is shifted into the bursting oscillations when $g_{NaP} = 0.41 \text{ mS/cm}^2$. This scenario presents a bursting with fast, low-amplitude spikes whose amplitude first declines and afterward raises until the end of bursting (Golomb et al., 2006). In our simulations, the depressed I_{KM} also increases the spike amplitude and reduces the spike frequency with time, but does not stop the bursting. Then, in the last stage the I_{pump} continues this process reaching the saddle homoclinic orbit bifurcation point where the system jumps to the resting state. Modulating effects of I_{pump} are also observed in the transition to SD. With the interruption of I_{pump} , there is a large augment of $[K^+]_o$. Hence, the depressed K^+ currents can not maintain the spikes, changing the system behavior to a slow depolarization wave. At the end, the membrane is repolarized by I_{pump} via a fold bifurcation. Therefore, in our simulations with high $[K^+]_o$ and zero $[Ca^{2+}]_o$ when the K^+ currents are depressed and synaptic transmission are blocked, the Na^+-K^+ pump is the main mechanism in the modulation of neuronal behavior.

5.3. Mechanistic similarity between ictal bursting and SD

In spite of the differences between epilepsy and migraine, they are comorbid-distinct health conditions in the same individual (Aguggia et al., 2007). In some cases, headaches are following epileptic attacks and seizures cause a syndrome similar to the headache phase of migraine in 50% of epileptics (Gorji, 2001). Moreover, some antiepileptic drugs are effective therapies for both epilepsy and migraine prevention, suggesting that these conditions arise from a common brain state wherein an abnormally increased neuronal excitability is observed (Welch, 2005). Thus, there may be an underlying mechanistic similarity common to both disorders that induces the increased neuronal excitability (Kager et al., 2000).

In this work, high $[K^+]_o$ and zero $[Ca^{2+}]_o$ present favorable conditions for the occurrence of ictal bursting and SD. This situation depresses the inhibitory mechanisms, raising the neuronal excitability. Here, the augment of $[K^+]_o$ changes the neuron behavior. At high $[K^+]_o$, it is possible to elicit ictal bursting without any external stimulus and, above the “ceiling” level, the system bifurcates from bursting to SD. On the other hand, the Na^+-K^+ pump modulates their dynamic behaviors. In both cases, this is the mechanism responsible for the cell repolarization. Therefore, the results denote that specific mechanisms may be able to alter the neuronal excitability in both disorders.

6. Conclusion

For the advance in the investigations of more effective drugs and therapies, it is crucial to better understand the underlying causes of neurological diseases. However, due to their complex dynamics, mathematical models with biological plausibility have presented considerable insight into how the cellular mechanisms produce abnormal oscillatory patterns within these neurological conditions. Using a model of hippocampal region CA1, our simulations reproduce with high $[K^+]_{bath}$ (8 mM/l) and zero $[Ca^{2+}]_{bath}$ seizure-like discharges (ictal bursting) without any external stimuli and the transition to spreading depression by the interruption of the Na^+-K^+ pump activity. Important regulatory mechanisms of ion concentration were added in the Golomb model. Herewith, we analyzed the consequences of high $[K^+]_o$ in the interactions between the ionic currents. Based on the fast-slow method, it was possible to verify the effects of $[K^+]_o$ and I_{pump} on the neuronal behavior, understanding the transitions to different stages of the ictal bursting and SD. These studies are consistent with data from hippocampal slices where increasing neuronal excitability is caused by high $[K^+]_o$ while the Na^+-K^+ pump modulates the neuronal behavior (Jensen and Yaari, 1997). Based on experimental evidences that still need theoretical explanations, this work suggests how the $[K^+]_o$ dynamics may raise the cellular excitability and influence the neuronal behaviors in the different stages of seizure discharges and SD. Nevertheless, other mechanisms may also change the neuronal excitability such as gap junctions, cellular volume variations, excitatory and inhibitory synapses. Hence, further studies involving all these mechanisms are important to provide new insights into how the neuron works within these neurological conditions. Moreover, additional studies concerning the global behavior of the network are necessary to better understand the epileptiform synchronization and the propagation of SD wave through the network.

Acknowledgments

The work was supported by the Brazilian agencies Conselho Nacional de Desenvolvimento Científico e Tecnológico (CNPq), Coordenação de Aperfeiçoamento de Pessoal de Nível Superior (CAPES), the German agency Deutscher Akademischer Austausch Dienst (DAAD) and BioSim (EU) contract no. LSHB-CT-2004-005137. The authors are grateful to Dr. D. Golomb for the information about his neuron model.

References

- Aguggia, M., D'Andrea, G., Bussone, G., 2007. Neurophysiology and neuromodulators. *Neurol. Sci.* 28, S97–S100.
- Almeida, A.C.G., Rodrigues, A.M., Scorza, F.A., Cavalheiro, E.A., Teixeira, H.Z., Duarte, M.A., Silveira, G.A., Arruda, E.Z., 2008. mechanistic hypotheses for nonsynaptic epileptiform activity induction and its transition from the interictal to ictal state-computational simulation. *Epilepsia* 49, 1908–1924.

- Amzica, F., Massimini, M., Manfredi, A., 2002. Spatial buffering during slow and paroxysmal sleep oscillations in cortical networks of glial cells in vivo. *J. Neurosci.* 22, 1042–1053.
- Bazhenov, M., Timofeev, I., Steriade, M., Sejnowski, T.J., 2004. Potassium model for slow (2–3 Hz) in vivo neocortical paroxysmal oscillations. *J. Neurophysiol.* 92, 1116–1132.
- Benarroch, E.E., 2005. Neuron–astrocyte interactions: partnership for normal function and disease in the central nervous system. *Mayo Clin. Proc.* 80, 1326–1338.
- Bertram, R., Butte, M.J., Kiemel, T., Sherman, A., 1995. Topological and phenomenological classification of bursting oscillations. *Bull. Math. Biol.* 57, 413–439.
- Bikson, M., Ghai, R.S., Baraban, S.C., Durand, D.M., 1999. Modulation of burst frequency, duration, and amplitude in the zero- Ca^{2+} model of epileptiform activity. *J. Neurophysiol.* 82, 2262–2270.
- Borck, C., Jefferys, J.G.R., 1999. Seizure-like events in disinhibited ventral slices of adult rat hippocampus. *J. Neurophysiol.* 82, 2130–2142.
- Cohen, J.E., Fields, R.D., 2004. Extracellular calcium depletion in synaptic transmission. *Neuroscientist* 10, 12–17.
- Dahlem, M.A., Chroniclec, E.P., 2004. A computational perspective on migraine aura. *Prog. Neurobiol.* 74, 351–361.
- D'Ambrosio, R., 2004. The role of glial membrane ion channels in seizures and epileptogenesis. *Pharmacol. Ther.* 103, 95–108.
- D'Ambrosio, R., Gordon, D.S., Winn, H.R., 2002. Differential role of KIR channel and Na^+/K^+ -pump in the regulation of extracellular K^+ in rat hippocampus. *J. Neurophysiol.* 87, 87–102.
- Dichter, M.A., Herman, C.J., Selzer, M., 1972. Silent cells during interictal discharges and seizures in hippocampal penicillin foci. Evidence for the role of extracellular K^+ in the transition from the interictal state to seizures. *Brain Res.* 48, 173–183.
- Ermentrout, G.B., 2002. *Simulating, Analyzing, and Animating Dynamical Systems: A Guide to Xppaut for Researchers and Students (Software, Environment, Tools)*. Society for Industrial and Applied Mathematics, Philadelphia, PA, USA.
- Feldberg, W., Sherwood, S.L., 1957. Effects of calcium and potassium injected into the cerebral ventricles of the cat. *J. Physiol.* 139, 408–416.
- Feng, Z., Durand, D.M., 2006. Effects of potassium concentration on firing patterns of low-calcium epileptiform activity in anesthetized rat hippocampus: inducing of persistent spike activity. *Epilepsia* 47, 727–736.
- Fertziger, A.P., Ranck, J.B., 1970. Potassium accumulation in interstitial space during epileptiform seizures. *Exp. Neurol.* 26, 571–585.
- Fisher, R.S., Pedley, T.A., Prince, D.A., 1976. Kinetics of potassium movement in normal cortex. *Brain Res.* 101, 223–237.
- Frankenhaeuser, B., Hodgkin, A.L., 1956. The after-effects of impulses in the giant nerve fibers of Loligo. *J. Physiol.* 131, 341–376.
- Fröhlich, F., Bazhenov, M., 2006. Coexistence of tonic firing and bursting in cortical neurons. *Phys. Rev. E* 74, 031922.
- Fröhlich, F., Bazhenov, M., Timofeev, I., Steriade, M., Sejnowski, T.J., 2006. Slow state transitions of sustained neural oscillations by activity-dependent modulation of intrinsic excitability. *J. Neurosci.* 26, 6153–6162.
- Golomb, D., Yue, C., Yaari, Y., 2006. Contribution of persistent Na^+ current and M-type K^+ current to somatic bursting in CA1 pyramidal cells: combined experimental and modeling study. *J. Neurophysiol.* 96, 1912–1926.
- Gorji, A., 2001. Spreading depression: a review of the clinical relevance. *Brain Res.* 38, 33–60.
- Grafstein, B., 1956. Mechanism of spreading cortical depression. *J. Neurophysiol.* 19, 154–171.
- Green, J.D., 1964. The hippocampus. *Physiol. Rev.* 44, 561–608.
- Haglund, M.M., Schwartzkroin, P.A., 1990. Role of Na^+/K^+ pump potassium regulation and IP_3 s in seizures and spreading depression in immature rabbit hippocampal slices. *J. Neurophysiol.* 63, 225–239.
- Heinemann, U., Konnerth, A., Pumain, R., Wadman, W., 1986. Extracellular calcium and potassium concentration changes in chronic epileptic brain tissue. *J. Adv. Neurol.* 44, 641–661.
- Heinemann, U., Lux, H.D., Gutnick, M.J., 1977. Extracellular free calcium and potassium during paroxysmal activity in the cerebral cortex of the cat. *Exp. Brain Res.* 27, 237–243.
- Herreras, O., Somjen, G.G., 1993. Analysis of potential shifts associated with recurrent spreading depression and prolonged unstable spreading depression induced by microdialysis of elevated K^+ in hippocampus of anesthetized rats. *Brain Res.* 610, 283–294.
- Herreras, O., Somjen, G.G., Strong, A., 2005. Electrical prodromals of spreading depression void Grafstein's potassium hypothesis. *J. Neurophysiol.* 94, 3656–3657.
- Hoppensteadt, F.C., Izhikevich, E.M., 1997. *Weakly Connected Neural Networks*. Springer, New York.
- Izhikevich, E.M., 2007. *Dynamical Systems in Neuroscience: The Geometry of Excitability and Bursting*. MIT Press, Cambridge, MA.
- Jensen, M.S., Yaari, Y., 1997. Role of intrinsic burst firing, potassium accumulation, and electrical coupling in the elevated potassium model of hippocampal epilepsy. *J. Neurophysiol.* 77, 1224–1233.
- Jensen, M.S., Yaari, Y., 1988. The relationship between interictal and ictal paroxysms in an in vitro model of focal hippocampal epilepsy. *Ann. Neurol.* 24, 591–598.
- Kager, H., Wadman, W.J., Somjen, G.G., 2000. Simulated seizures and spreading depression in a neuron model incorporating interstitial space and ion concentrations. *J. Neurophysiol.* 84, 495–512.
- Kager, H., Wadman, W.J., Somjen, G.G., 2007. Seizure-like afterdischarges simulated in a model neuron. *J. Comput. Neurosci.* 22, 105–128.
- Kandel, E.R., Schwartz, J.H., Jessel, T.M., 2000. *Principles of Neural Science*. McGraw-Hill, New York, pp. 912–935.
- Konnerth, A., Heinemann, U., Yaari, Y., 1984. Slow transmission of neural activity in hippocampal area CA1 in absence of active chemical synapses. *Nature* 307, 69–71.
- Korn, S.J., Giacchino, J.L., Chamberlin, N.L., Dingledine, R., 1987. Epileptiform burst activity induced by potassium in the hippocampus and its regulation by GABA-mediated inhibition. *J. Neurophysiol.* 57, 325–340.
- Leão, A.A.P., 1944. Spreading depression of activity in the cerebral cortex. *J. Neurophysiol.* 7, 359–390.
- Leschinger, A., Stabel, J., Igelmund, P., Heinemann, U., 1993. Pharmacological and electrographic properties of epileptiform activity induced by elevated K^+ and lowered Ca^{2+} and Mg^{2+} concentration in rat hippocampal slices. *Exp. Brain Res.* 96, 230–240.
- Lian, J., Bikson, M., Shuai, J., Durand, D.M., 2001. Propagation of nonsynaptic epileptiform activity across lesion in rat hippocampal slices. *J. Physiol.* 537, 191–199.
- Lux, H.D., 1974. The kinetics of extracellular potassium relation to epileptogenesis. *Epilepsia* 15, 375–393.
- Martins-Ferreira, H., Nedergaard, M., Nicholson, C., 2000. *Brain Res. Rev.* 32, 215–234.
- McCormick, D.A., Contreras, D., 2001. On the cellular and network bases of epileptic seizures. *Annu. Rev. Physiol.* 63, 815–846.
- Moody, W.J., Futamachi, K.J., Prince, D.A., 1974. Extracellular potassium during epileptogenesis. *Exp. Neurol.* 42, 248–263.
- Müller, M., Somjen, G.G., 2000. Na^+ and K^+ concentrations, extra- and intracellular voltages, and the effect of TTX in hypoxic rat hippocampal slices. *J. Neurophysiol.* 83, 735–745.
- Nicholson, C., 1980. Modulation of extracellular calcium and its functional implications. *Fed. Proc.* 39, 1519–1523.
- Pan, E., Stringer, J.L., 1997. Role of potassium and calcium in the generation of cellular bursts in the dentate gyrus. *J. Neurophysiol.* 77, 2293–2299.
- Park, E.H., Durand, D.M., 2006. Role of potassium lateral diffusion in non-synaptic epilepsy: a computational study. *J. Theor. Biol.* 238, 666–682.
- Pumain, R., Menini, C., Heinemann, U., Louvel, J., Silva-Barrat, C., 1985. Chemical synaptic transmission is not necessary for epileptic seizures to persist in the baboon papio papio. *Exp. Neurol.* 89, 250–258.
- Somjen, G.G., 1979. Extracellular potassium in the mammalian central nervous system. *Annu. Rev. Physiol.* 41, 159–177.
- Somjen, G.G., 2001. Mechanisms of spreading depression and hypoxic spreading depression-like depolarization. *Physiol. Rev.* 81, 1065–1096.
- Somjen, G.G., 2002. Ion regulation in the brain: implications for pathophysiology. *Neuroscientist* 8, 254–267.
- Somjen, G.G., Aitken, P.G., Czéh, G.L., Herreras, O., Jing, J., Young, J.N., 1992. Mechanisms of spreading depression: a review of recent findings and a hypothesis. *Can. J. Physiol. Pharmacol.* 70 (Suppl. S), 248–254.
- Somjen, G.G., Aitken, P.G., Giacchino, J.L., McNamara, J.O., 1985. Sustained potential shifts and paroxysmal discharges in hippocampal formation. *J. Neurophysiol.* 53, 1079–1097.
- Takano, T., Tian, G.F., Peng, W., Lou, N., Lovatt, D., Hansen, A.J., Kasischke, K.A., Nedergaard, M., 2007. Cortical spreading depression causes and coincides with tissue hypoxia. *Nat. Neurosci.* 10, 754–762.
- Teixeira, H.Z., Almeida, A.C.G., Infantesi, A.F.C., Rodrigues, A.M., Costa, N.L., Duarte, M.A., 2008. Identifying essential conditions for refractoriness of Leão's spreading depression-Computational modelling. *Comp. Bio. Chemist., V.x*, P.x-xx. doi:10.1016/j.compbiolchem.2008.03.011.
- Traynelis, S.F., Dingledine, R., 1988. Potassium-induced spontaneous electrographic seizures in the rat hippocampal slice. *J. Neurophysiol.* 59, 259–276.
- Welch, K.M., 2005. Brain hyperexcitability: the basis for antiepileptic drugs in migraine prevention. *Headache* 45 (Suppl. 1), S25–S32.
- Xiong, Z.Q., Stringer, J.L., 2001. Prolonged bursts occur in normal calcium in hippocampal slices after raising excitability and blocking synaptic transmission. *J. Neurophysiol.* 86, 2625–2628.
- Zuckermann, E.C., Glaser, G.H., 1968. Hippocampal epileptic activity induced by localized ventricular perfusion with high-potassium cerebrospinal fluid. *Exp. Neurol.* 20, 87–110.